

Impurities in a Biased Graphene Bilayer

Johan Nilsson and A. H. Castro Neto

Department of Physics, Boston University, 590 Commonwealth Avenue, Boston, MA 02215

(dated: March 23, 2024)

We study the problem of impurities and mid-gap states in a biased graphene bilayer. We show that the properties of the bound states, such as localization lengths and binding energies, can be controlled externally by an electric field effect. Moreover, the band gap is renormalized and impurity bands are created at finite impurity concentrations. Using the coherent potential approximation we calculate the electronic density of states and its dependence on the applied bias voltage.

PACS numbers: 81.05.Jw 73.21.Ac 73.20.Hb

The discovery of single layer graphene [1], and its further experimental characterization demonstrating unconventional metallic properties [2, 3], have attracted a lot of attention in the condensed matter community. The graphene bilayer, which is made out of two stacked graphene planes, is a particularly interesting form of two-dimensional (2D) carbon because of its unusual physics that has its origins on the peculiar band structure. At low energies and long wavelengths it can be described in terms of massless, chiral, Dirac particles. Previous studies of the graphene bilayer have focused on the integer quantum Hall effect [4, 5], the effect of electron-electron interactions [6], and transport properties [7, 8, 9, 10, 11]. An important property of this system is that when an electric field is applied between the two graphene layers, an electronic gap opens in the spectrum [4, 12, 13]; the resulting system is called the biased graphene bilayer (BGB). In contrast, the single layer graphene does not have this unique property since to generate a gap in the electronic spectrum the sub-lattice symmetry of the honeycomb lattice has to be broken, and this is a costly energetic process.

Ohta et al. have studied graphene films on SiC substrates using angle-resolved photoemission spectroscopy (ARPES) [14], and spectra reminiscent of the BGB were uncovered. Nevertheless, the graphene films are heavily doped by the SiC and the chemical potential and gap value cannot be controlled independently. More recently, Castro et al. reported the first observation of a tunable electronic gap in a BGB through magnetotransport measurements of micro-mechanically cleaved graphene on a SiO₂ substrate [15]. By chemically doping the upper graphene layer with NH₃, it was shown that the BGB behaves as a semiconductor with a tunable electronic gap that can be changed from zero to a value as large as 0.3 eV by using fields of < 1 V/nm (below the electric breakdown of SiO₂). The importance of controlling both the chemical potential and the value of the electronic gap in a semiconductor cannot be overstated since it can open doors for a large number of applications, from transistors [16] to photo-detectors and lasers tunable by the electric field effect.

In order to understand and control the electronic prop-

erties of the BGB it is important to understand the effects of the unavoidable disorder. In this letter we show that bound states exist for arbitrary weak impurity potentials, and that their properties, such as binding energies and localization lengths, can be externally controlled with a gate bias. Moreover, we obtain the wave-functions of the mid-gap states, from which we derive a simple criterion for when the overlap between wavefunctions becomes important. This overlap results in band gap renormalization and possibly band tails extending into the gap region, as in the case of ordinary heavily doped semiconductors [17], or impurity bands for deep impurities. Unlike ordinary semiconductors, the electronic density of states can be completely controlled via the electric field effect. The impurity interaction problem is studied within the coherent potential approximation (CPA).

The Model. The low-energy effective bilayer Hamiltonian has the form [12, 13] (we use units such that $\hbar = 1$):

$$H_0(\mathbf{k}) = \begin{pmatrix} k_x + V\tau_z & t_z(1 + \tau_z) \\ t_z(1 - \tau_z) & -k_x - V\tau_z \end{pmatrix}; \quad (1)$$

where $\mathbf{k} = (k_x, k_y)$ is the 2D momentum measured relative to the K-point in the Brillouin zone (BZ), V is the potential energy difference between the two planes, $t_z = 0.35$ eV is the inter-layer hopping energy, and τ_i ($i = x, y, z$) are Pauli matrices. We choose units such that the Fermi Dirac velocity, v_F , is set to unity ($v_F = 3ta/2$ where $t = 3$ eV is the nearest neighbor hopping energy, and $a = 1.4$ Å is the lattice spacing). The corresponding spinor has weight on the different sublattices according to $\psi = (A_1; B_1; A_2; B_2)^T$ [6]. Solving for the spectrum of (1) one finds two pairs of electron-hole symmetric bands:

$$E^2 = k^2 + V^2 = 4 + t_z^2 = 2 \frac{q}{(V^2 + t_z^2)k^2 + t_z^4} = 4; \quad (2)$$

For the two bands closest to zero energy near the band edge (valence and conduction bands) one can write the spectrum as: $E_p(\mathbf{k}) = E_g/2 + (\mathbf{k} - \mathbf{k}_g)^2/(2m_g)$. Here $E_g = Vt_z = \sqrt{V^2 + t_z^2}$ is the energy gap, $\mathbf{k}_g = V/2 \frac{1}{1 + t_z^2} = \frac{V}{\sqrt{V^2 + t_z^2}}$ is a momentum shift, and m_g is an effective mass. Due to the non-zero \mathbf{k}_g the system is effectively one-dimensional (1D) near the band edge [13].

Dirac delta potentials. True bound states must lie inside of the gap so that their energies fulfill $|E_j| < E_g/2$. For a single local impurity the Green's function can be written as $G = G^0 + G^0 T G^0$ using the standard matrix approach [18], where the bare Green's function is $G^0 = (\epsilon - H_0)^{-1}$. The Fourier transform of a Dirac delta potential is $U = N \delta_{ij}$ (N being the number of unit cells) leading to $T = (U - N)^{-1} = (1 - U \bar{G}_j^0)^{-1}$. Here $i, j = (A, B)$ and $j = (1, 2)$ label the lattice site of the impurity. The quantity $\bar{G}_j^0(\epsilon) = \frac{1}{N} \sum_{\mathbf{k}} G_{0j}^0(\epsilon; \mathbf{k})$ is the local propagator at the impurity site and the momentum sum is over the whole BZ. Bound states are then identified by the additional poles of the Green's function due to the potential, these are given by $\bar{G}_j^0(\epsilon) = 1/U$. For energies inside of the gap we find:

$$\bar{G}_{A1}^0 = \frac{V=2}{2^2} \log \frac{4}{M^4 + (V^2=4 + \epsilon^2)^2} - \frac{2! V^h}{M^2} \tan^{-1} \frac{V^2=4 + \epsilon^2}{M^2} + \tan^{-1} \frac{2}{M^2}; \quad (3)$$

$$\bar{G}_{B1}^0 = \bar{G}_{A1}^0 - \frac{(V=2 + \epsilon^2) t_2^h}{M^2} \tan^{-1} \frac{V^2=4 + \epsilon^2}{M^2} + \tan^{-1} \frac{2}{M^2};$$

where $M^2 = \sqrt{V^2 t_2^2 + 4 - \epsilon^2 (V^2 + t_2^2)}$, and ϵ (7 eV) is a high energy cut-off [7]. The corresponding expressions in plane 2 are obtained by the substitution $V \rightarrow V$. From this we conclude that a Dirac delta potential always generates a bound state since \bar{G}^0 diverges as the band edge is approached (where $M \rightarrow 0$). The dependence on the cut-off (except for the overall scale) is rather weak so that the linear in-plane approximation to the spectrum should be a good approximation as in the case of graphene [19]. For a given strength of the potential U , there are four different bound state energies depending on which lattice site it is sitting on. In Fig. 1 we show the binding energy as a function of U and V for the deepest bound state. In the limit of $U \rightarrow 1$ the particle-hole symmetry of the bound state energies is restored. We will only consider attractive potentials in this work, analogous results will hold for repulsive potentials because of the particle-hole symmetry of the model. For smaller values of the potential ($|U| < 1$) the binding energy measured from the band edge: $E_b = E_g/2$ grows as U^2 and the states are weakly bound. For example, for $V = 40$ meV and $U < 1$ eV one finds $E_b < 4 \cdot 10^{-4} E_g$.

Angular momentum states. For any potential with cylindrical symmetry it is useful to classify the eigenstates according to their angular momentum m . The real-space version of (1) in polar coordinates is obtained by the substitutions $k_x \rightarrow ik_r$, $k_y \rightarrow i(\partial_r - \partial_\theta)$, $\partial_x \rightarrow \partial_r \cos \theta - \partial_\theta \sin \theta$, $\partial_y \rightarrow \partial_r \sin \theta + \partial_\theta \cos \theta$. Adding a potential that only depends on the radial coordinate r one can (in analogy with the usual Dirac equation [20]) construct an angular momentum operator that commutes with the Hamiltonian.

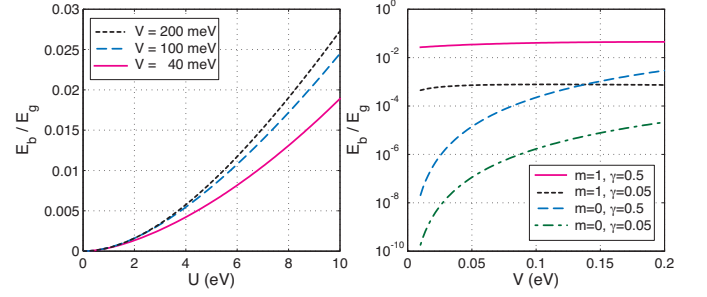


FIG. 1: (Color online) Left: Bound state binding energies E_b (in units of the gap E_g) for a Dirac delta potential of strength U for different bias V . Right: Binding energy of a potential well of range $R = 10$ a and strength $V = 1$ eV for different angular momentum m .

The angular (θ) dependence of the angular momentum m eigenstates are those of the vector:

$$u_{\mu m}(\theta) = e^{im\theta} \begin{pmatrix} 1 \\ i e^{i\theta} e^{-i\theta/2} \\ 1 \\ i e^{i\theta} e^{-i\theta/2} \end{pmatrix}^T; \quad (4)$$

The parameter γ is introduced for later convenience. If the potential generates bound states inside of the gap these states decay exponentially: $\sim e^{-r}$. Assuming that the potential decays fast enough, the asymptotic behavior of (1) implies that the allowed values of γ are

$$\gamma = \frac{1}{2} \frac{1}{(2 + V^2=4) - iM^2}; \quad (5)$$

so that weakly bound states have a localization length

$$l = \frac{1}{2k_g} = \frac{1}{2\sqrt{V^2 t_2^2 - E_g^2}}; \quad (6)$$

that diverges as the band edge is approached and decreases with increasing bias voltage.

Free particle wave-functions. The free particle wave-functions in the angular momentum basis can be conveniently expressed in terms of the following vectors:

$$v_{z\mu m}(z) = \begin{pmatrix} Z_m(z) \\ Z_{m-1}(z) \\ Z_m(z) \\ Z_{m+1}(z) \end{pmatrix}^T; \quad (7)$$

$$w(p) = \begin{pmatrix} 0 \\ (\epsilon + V=2)^2 - p^2 \\ (\epsilon + V=2)^2 - p^2 \\ t_2^2 (\epsilon^2 - V^2=4) \end{pmatrix} \begin{pmatrix} 1 \\ -V=2 \\ p \\ C \\ A \end{pmatrix}; \quad (8)$$

The last vector is useful as long as $\epsilon \neq V=2$. The function determining the eigenstates is: $D(p; \epsilon) = p^2 - V^2=4 - \epsilon^2 + V^2 t_2^2 = 4 - \epsilon^2 (V^2 + t_2^2)$. Then, provided that $D(k; \epsilon) = 0$, ($k > 0$) which corresponds to propagating modes, the eigenfunctions are proportional to $v_{z\mu m}(\epsilon; k; r) = u_{1\mu m} \cdot v_{z\mu m}(kr) \cdot w(k)$; where $Z_m(z) = J_m(z)$ or $Y_m(z)$ are Bessel functions. The star product of two vectors is a vector with components defined by

$[a \otimes b]_j = a_j b_j$. If on the other hand $D(i;!) = 0$, ($\text{Re}[j] > 0$) the eigenfunctions are:

$$\begin{aligned} K_{j,m}(!; ;r) &= u_{0,j,m} \otimes v_{K,j,m}(r) \otimes w(!; i); \\ I_{j,m}(!; ;r) &= u_{0,j,m} \otimes v_{I,j,m}(r) \otimes w(!; i); \end{aligned} \quad (9)$$

with $I_m(z)$ and $K_m(z)$ being modified Bessel functions. That these vectors are eigenstates can be verified directly by applying the real space version of (1) to them.

Local impurity wave-functions. The bound state wave-functions can be read off from the t-matrix equation. For a Dirac delta potential the resulting wave-functions are proportional to the propagator from the site of the impurity to the site of interest evaluated at the energy of the bound state. These propagators are easily expressed in terms of the free-particle wavefunctions, e.g.:

$$\begin{aligned} G_{j,A1} &= \frac{h}{i2M^2} \frac{K_{j,0}(!; +; r) K_{j,0}(!; ; r)}{K_{j,0}(!; ; r)} i; \\ G_{j,B1} &= \frac{h}{2M^2} \frac{K_{j,1}(!; +; r) K_{j,1}(!; ; r)}{K_{j,1}(!; ; r)} i; \end{aligned} \quad (10)$$

There are also analogous contributions coming from the other valley. The asymptotic behavior of the modified Bessel functions $K_n(z) \sim \exp(-z)$ as $z \rightarrow \infty$ implies that the bound states are exponentially localized on a scale that is the same as in the general consideration above in (5) and (6). At short distances one may use that $K_n(z) \sim 1/z^n$ for $n \rightarrow 1$ to conclude that the wave-functions are not normalizable in the continuum. The divergence is however not real since in a proper treatment of the short-distance physics it is cut off by the lattice spacing a . The characteristic size of the wave-functions allows for a simple estimate of the critical density of impurities n_c above which the overlap, and hence the interaction between the impurities, becomes important. For weakly bound states we estimate $n_c \sim [V t_2 = (k_g t)^2 = (2/\bar{v})^2 (E_b = E_g)]$; indicating that the critical density increases with the applied gate voltage. For $V \sim t_2$ we find $n_c \sim 2.5 \cdot 10^3 (E_b = E_g)$, and for $U < 1 \text{ eV}$ one has $n_c < 10^6$. This result shows that even a small amount of impurities can have strong effects in the electronic properties of the BGB.

Variational approach. A simple variational wave-function consisting of a wave-packet with angular momentum m and a momentum close to k_g from the E_+ band is: $\text{var}(!) = \int_{k_g}^{R_{k_g}+} dp \otimes J_{j,m}(E_+(p); p; r) \otimes p$; where we assume that k_g . A variational calculation shows that for any m , a weak attractive potential of strength $-U$ leads to a weakly bound state with binding energy $E_b \sim U^2$. This can be understood by noting that for each value of m , due to k_g being non-zero, the problem maps into a 1D system with an effective local potential, and in 1D a weak attractive potential ($-U$) always leads to a bound state with binding energy $E_b \sim U^2$. Thus the result is a direct consequence of the peculiar topology of the BGB band edge [21].

Potential well. The free-particle solutions can be used to study a simple BGB potential well modeled by two potentials: $g_j = \gamma_j (R - r) \otimes R$. is the Heaviside step function so that R is the size of the well and γ_j its dimensionless strength in plane j . Bound states of the potential well are then described by two $K_{j,m}$ outside and the appropriate pair of $J_{j,m}$'s and $I_{j,m}$'s inside of the well. By matching the wave-functions at $r = R$ we have studied the binding energies and find that the deepest bound states are in one of the angular momentum channels $m = 0; \pm 1$ for a substantial parameter range. Since these types of states are also present for the Dirac delta potential we argue that the physics of short-range potentials can be approximated (except for the short-distance physics) by Dirac delta potentials with a strength tuned to give the correct binding energy. A typical result for the binding energies is shown in Fig. 1. The important case of a screened Coulomb potential generally requires a more sophisticated approach. Nevertheless, we do not anticipate any qualitative discrepancies between a potential well and a screened Coulomb potential. We expect the screening wave-vector to be roughly proportional to the density of states at the Fermi energy; and once the range and the strength of the potential have been estimated a potential well can be used to estimate the binding energies. We also note that the asymptotic behavior in (5) is quite general for a decaying potential.

Coherent potential approximation. As discussed above, for a finite density n_i of impurities the bound states interact with each other leading to the possibility of band gap renormalization and the formation of impurity bands. A simple theory of these effects is the CPA [22, 23]. In this approximation the disorder is treated as a self-consistent medium with recovered translational invariance. The medium is described by a set of four local self-energies which are allowed to take on different values on all of the inequivalent lattice sites. The self-energies are chosen so that on average there is no scattering in the effective medium. Explicitly we introduce the diagonal matrix $H(!) = D \text{diag} \{A_1; B_1; A_2; B_2\}$; here and in the following we suppress the frequency-dependence of the self-energies for brevity. Then the Green's function matrix is given by

$$G^{-1}(!; k) = ! \otimes H_0(k) \otimes H(!); \quad (11)$$

Finally, following the standard approach to derive the CPA [18, 23], we obtain the self-consistent equations: $\gamma_j = n_i U = 1 \otimes (U \otimes \gamma_j) \otimes G_j$; Using the propagators obtained from (11) it is straightforward to compute G using the same approximations that lead to (3). From these equations one can obtain the density of states (DOS) on the different sublattices: $\gamma_j(!) = \text{Im} G_j(! + i) =$.

In the clean case one finds:

$$\begin{aligned} \rho_{A1}^0 &= \frac{1}{2} \frac{V^2}{V^2 + t_\perp^2} \frac{1}{V^2 t_\perp^2} \frac{1}{(V^2 + t_\perp^2)^{1/2}}; \\ \rho_{B1}^0 &= \rho_{A1}^0 + \frac{t_\perp^2}{2} \frac{1}{(V^2 + t_\perp^2)^{1/2}} \frac{1}{V^2 t_\perp^2} \frac{1}{(V^2 + t_\perp^2)^{1/2}}; \end{aligned} \quad (12)$$

for $j|j\rangle$ $E_g=2$. Here $\rho_{(0;1;2)}$ for $(j|j\rangle$ $V=2$, $V=2$ $j|j\rangle$ $t_\perp^2 + V^2=4$, $\rho_{(0;1;2)}$ $t_\perp^2 + V^2=4$ $j|j\rangle$. The corresponding quantities in plane 2 are obtained by the substitution $V \rightarrow -V$. Taking the limit $V \rightarrow 0$ we recover the unbiased result of Ref. 7. Notice the square-root singularity that starts to appear already above $V=2$.

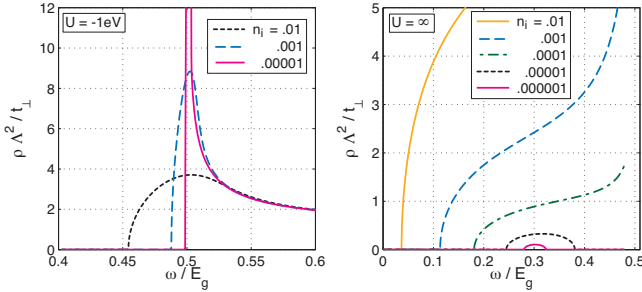


FIG. 2: (Color online) Left: DOS as a function of the energy (in units of E_g) close to the conduction band edge for different impurity concentrations (see inset), $U = -1$ eV. Right: Details of the DOS inside of the gap for different impurity concentrations for $U \rightarrow \infty$. In both cases $V = 40$ meV.

The numerically calculated density of states for $U \rightarrow \infty$ is shown in Fig. 2. The impurity band evolves from the single-impurity B2 bound state which for the parameters involved is located at $0.3E_g$. Further evidence for this interpretation is that the total integrated DOS inside the split-off bands for the two lowest impurity concentrations is equal to n_i . It is worth mentioning that the width of the impurity band in the CPA is likely to be overestimated. The reason for this is that the use of effective atoms, all of which have some impurity character, facilitates the interaction between the impurities [23]. For smaller values of the impurity strength the single-impurity bound states are all weakly bound (cf. Fig. 1) and the "impurity bands" merge with the bulk bands as shown in Fig. 2 and 3. The bands have been shifted rigidly by the amount $n_i U$ for a more transparent comparison between the different cases. The smoothening of the singularity as well as the band gap renormalization is apparent. Observe also that the band edge moves further into the gap at the side where the bound states are located. It is likely that the CPA gives a better approximation for these states since by (5) they are weakly damped almost propagating modes. Notice that the gap and the whole structure of the DOS in the region of the gap is changing with V , and in particular the possibility that the actual gap closes before $V = 0$ because of impurity-induced states inside of the gap.

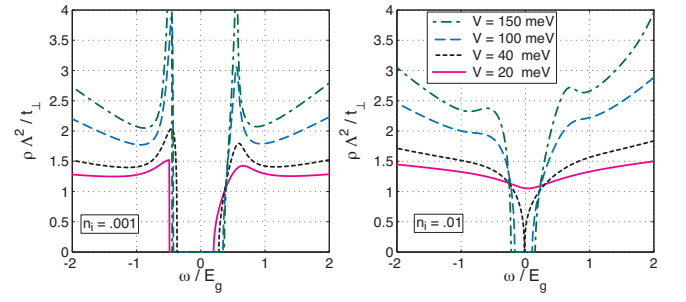


FIG. 3: (Color online) DOS as a function of energy (in units of E_g) for different values of the applied bias V (see inset) and $U = -10$ eV. Left: $n_i = 10^{-3}$; Right: $n_i = 10^{-2}$.

Conclusion. We have studied the effects of impurities in a biased graphene bilayer. We find that local potentials always generate bound states inside of the gap. A finite density of impurities can lead to the formation of impurity bands as well as band gap renormalization. We show that, unlike ordinary semiconductors, the electronic properties and density of states can be controlled externally via an applied voltage bias.

We thank A. Geim, F. Guinea and N.M.R. Peres for many illuminating discussions. A.H.C.N. is supported through NSF grant DMR-0343790.

-
- [1] K. S. Novoselov et al, Science 306, 666 (2004).
 - [2] K. S. Novoselov et al, Nature 438, 197 (2005).
 - [3] Y. Zhang et al, Nature 438, 201 (2005).
 - [4] E. M. McCann and V. I. Fal'ko, Phys. Rev. Lett. 96, 086805 (2006).
 - [5] K. S. Novoselov et al, Nature Physics 2, 177 (2006).
 - [6] J. Nilsson et al, Phys. Rev. B 73, 214418 (2006).
 - [7] J. Nilsson et al, Phys. Rev. Lett. 97, 266801 (2006).
 - [8] M. Koshino and T. Ando, Phys. Rev. B 73, 245403 (2006).
 - [9] M. I. Katsnelson, Eur. Phys. J. B 52, 151 (2006).
 - [10] I. Snymán and C. W. J. Beenakker, Phys. Rev. B 75, 045322 (2007).
 - [11] D. S. L. Abergel and V. I. Fal'ko, cond-mat/0610673.
 - [12] E. M. McCann, Phys. Rev. B 74, 161403 (2006).
 - [13] F. Guinea, A. H. Castro Neto, and N. M. R. Peres, Phys. Rev. B 73, 245426 (2006).
 - [14] T. Ohta et al, Science 313, 951 (2006).
 - [15] E. V. Castro et al, cond-mat/0611342.
 - [16] J. Nilsson and et al, cond-mat/0607343.
 - [17] P. Van Mieghem, Rev. Mod. Phys. 64, 755 (1992).
 - [18] W. Jones and N. H. March, Theoretical solid state physics, vol. 2 (Dover, New York, 1985).
 - [19] T. O. Wehling et al, cond-mat/0609503.
 - [20] D. P. DiVincenzo and E. J. Mele, Phys. Rev. B 29, 1685 (1984).
 - [21] This feature is unstable to the perturbation of the trigonal warping term ϵ_3 [6]. The effect of ϵ_3 is large for small bias and leads to an elliptic dispersion at the band edge. We do not expect ϵ_3 to alter our results for strong

in purity potentials and large in purity concentrations.

175, 747 (1968).

[22] P. Soven, Phys. Rev. 156, 809 (1967).

[23] B. Velicky, S. Kirkpatrick, and H. Ehrenreich, Phys. Rev.